NASA TECHNICAL MEMORANDUM

NASA TM X-2466

NASA TM X-2466

BOUNDARY-LAYER TRANSITION DETECTION ON THE X-15 VERTICAL FIN USING SURFACE-PRESSURE-FLUCTUATION MEASUREMENTS

by Thomas L. Lewis and Richard D. Banner

Flight Research Center
Edwards, Calif. 93523

NATIONAL AERONAUTICS AND SPACE ADMINISTRATION • WASHINGTON, D. C. • DECEMBER 1971

1. Report No.	2. Government Accession No.	3. Recipient's Catalog No.
NASA TM X-2466		

4. Title and Subtitle	5. Report Date
BOUNDARY-LAYER TRANSITION DETECTION ON THE X-15 VERTICAL FIN USING SURFACE-PRESSURE-FLUCTUATION MEASUREMENTS	December 1971
	6. Performing Organization Code
7. Author(s)	8. Performing Organization Report No.
Thomas L. Lewis and Richard D. Banner	H-660
	10. Work Unit No.
9. Performing Organization Name and Address	126-61-14-00-24
NASA Flight Research Center P. O. Box 273 Edwards, California 93523	11. Contract or Grant No.
	13. Type of Report and Period Covered
12. Sponsoring Agency Name and Address	Technical Memorandum
National Aeronautics and Space Administration Washington, D. C. 20546	14. Sponsoring Agency Code

15. Supplementary Notes

16. Abstract

A flush-mounted microphone on the vertical fin of an X-15 airplane was used to investigate boundary-layer transition phenomenon during flights to peak altitudes of approximately 70,000 meters (230,000 feet). The flight results were compared with those from wind-tunnel studies, skin temperature measurements, and empirical prediction data. The Reynolds numbers determined for the end of transition were consistent with those obtained from wind-tunnel studies. Maximum surface-pressure-fluctuation coefficients in the transition region were about an order of magnitude greater than those for fully developed turbulent flow. This was also consistent with wind-tunnel data.

It was also noted that the power-spectral-density estimates of the surface-pressure fluctuations were characterized by a shift in power from high frequencies to low frequencies as the boundary layer changed from turbulent to laminar flow. Large changes in power at the lowest frequencies appeared to mark the beginning of transition.

17. Key Words (Suggested by Author(s))	18. Distribution Statement
Surface-pressure fluctuations Boundary-layer transition	Unclassified - Unlimited

19. Security Classif. (of this report)	20. Security Classif. (of this page)	21. No. of Pages	22. Price*
Unclassified	Unclassified	16	$3.00

*For sale by the National Technical Information Service, Springfield, Virginia 22151

BOUNDARY-LAYER TRANSITION DETECTION ON THE X-15 VERTICAL FIN USING SURFACE-PRESSURE-FLUCTUATION MEASUREMENTS

Thomas L. Lewis and Richard D. Banner
Flight Research Center

INTRODUCTION

Analysis of skin temperature measurements on the X-15 airplane fuselage and wings (refs. 1 and 2) indicated that surface irregularities were the most probable cause of early boundary-layer transition. Unfortunately, during flights to high altitude, it was difficult to determine the actual location of transition by skin temperature measurements alone, because of the low heating rates encountered while transition was taking place. As a result, alternative methods were sought to more accurately establish the occurrence of transition on these flights.

An analysis of data obtained from a flush-mounted microphone installed on the upper vertical fin as a part of investigations of "boundary-layer noise" revealed that large response changes were recorded at the time transition was believed to be taking place. Further studies were therefore conducted which indicated that microphone data might be used as an alternate method of determining the location of transition.

This paper describes the results and interpretation of microphone measurements of the transition phenomenon and compares the results with those obtained from wind-tunnel measurements.

SYMBOLS

Physical quantities in this report are given in the International System of Units and parenthetically in U. S. Customary Units. The measurements were taken in U. S. Customary Units. Factors relating the two systems are presented in reference 3.

f	frequency, Hz
g	gravitational conversion factor, $\frac{\text{kg-m}}{\text{N-sec}^2}\left(32.17\ \frac{\text{lbm-ft}}{\text{lbf-sec}^2}\right)$
h_p	altitude, m (ft)
M	Mach number

OASPL	overall sound pressure level, $10 \log_{10} \frac{\overline{P^2}}{P^2_{ref}}$, dB
$\hat{P}(f)$	estimated power spectral density of the sound pressure level, $10 \log_{10} \frac{\overline{P^2(f)}}{P^2_{ref}}$, dB/Hz
$\overline{P^2}$	mean square pressure, hN^2/m^4 (lbf^2/ft^4)
$\overline{P^2(f)}$	average mean square pressure in the octave band, hN^2/m^4 Hz (lbf^2/ft^4 Hz)
P^2_{ref}	acoustic sound power reference pressure, 4×10^{-14} hN^2/m^4 (1.74×10^{-3} lbf^2/ft^4)
$\frac{\sqrt{\overline{P^2}}}{q_l}$	root-mean-square pressure-fluctuation coefficient
q	dynamic pressure, hN/m^2 (lbf/ft^2)
R	local Reynolds number based on the distance from the leading edge, $\frac{\rho_l V_l x}{\mu_l g}$
$\frac{R}{x}$	local unit Reynolds number, $\frac{\rho_l V_l}{\mu_l g}$, m^{-1} (ft^{-1})
t	time, sec
V	velocity, m/sec (ft/sec)
x	distance measured from the leading edge, m (ft)
α	airplane angle of attack, deg
β	airplane angle of sideslip, deg
δ_v	vertical fin deflection, deg
μ	dynamic viscosity, N sec/m^2 (lbf sec/ft^2)
ρ	density of air, kg/m^3 (lbm/ft^3)

Subscripts:

l	local

max maximum

∞ free stream

EQUIPMENT AND INSTRUMENTATION

X-15 Airplane

The X-15 is a rocket-powered research vehicle which was launched at an altitude of about 13,700 meters (45,000 feet) from a pylon mounting below the right wing of a B-52 carrier aircraft. The X-15 was flown to altitudes of 108,000 meters (354,200 feet) and at speeds approaching Mach 6.0. A detailed description of the X-15 aircraft is included in reference 4, and a three-view drawing is provided in figure 1.

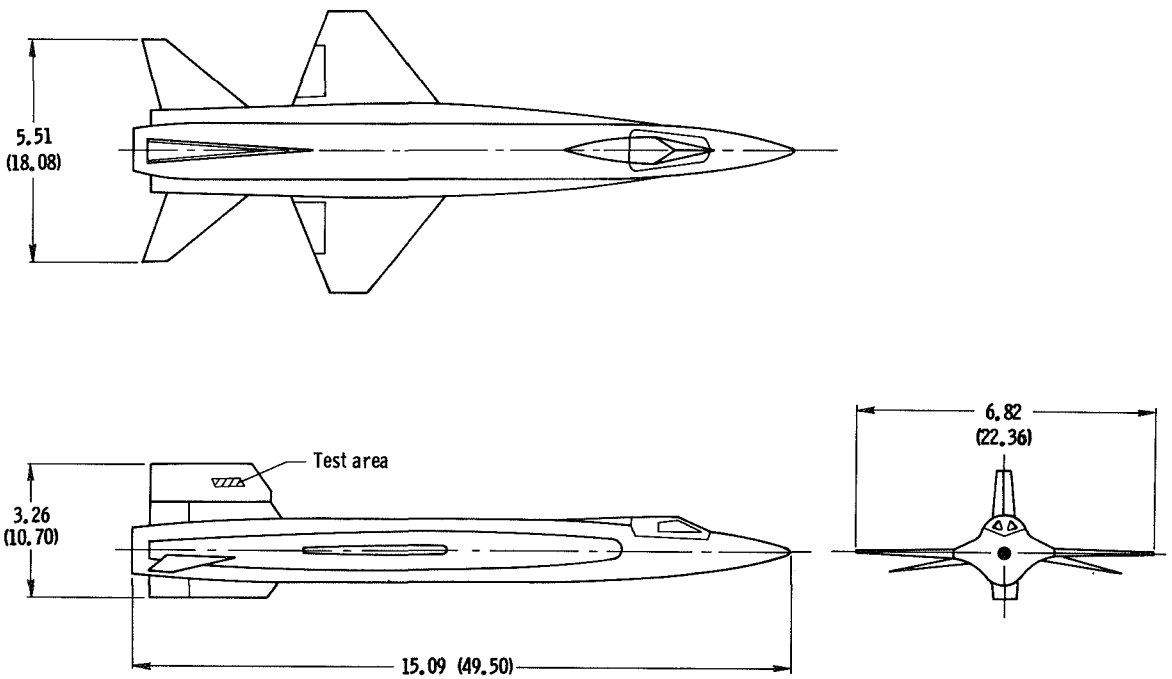

Figure 1. Three-view drawing of the basic X-15 airplane. Dimensions in meters (feet).

Vertical Fin

The modified X-15 vertical fin used in the heat transfer and skin friction investigations of reference 5 and 6 was used in the present tests. The leading edge of the fin had been modified to a "sharp," 0.038-centimeter (0.015-inch) radius to provide a uniform flow over the fin surface. A sketch of the fin is shown in figure 2. Boundary-layer trips approximately 2.5 millimeters (0.01 inch) in diameter and from 0.51 to 0.64 millimeter (0.02 to 0.025 inch) high were installed about 25 millimeters (1 inch) apart along a row parallel to and approximately 12.2 centimeters (4.8 inches) aft of the leading edge. This location is also the approximate chordwise position of the first of two rows of screws used to attach the sharp leading edge of the vertical fin. These

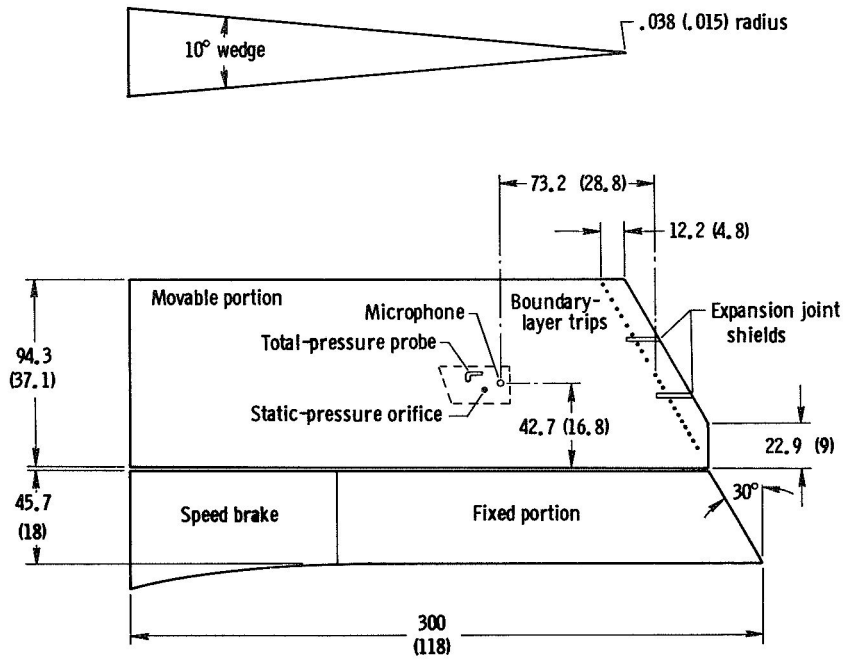

Figure 2. Sketch of vertical fin with sharp leading edge showing location of the boundary-layer trips, leading-edge expansion joint shields, and sensors. Dimensions in centimeters (inches). (Drawing not to scale.)

screw heads also protruded above the surface (fig. 3(a)), but not as much as the boundary-layer trips.

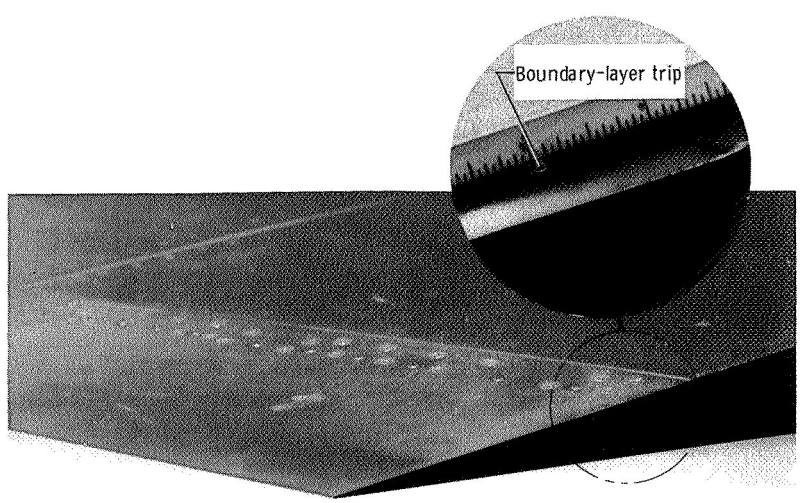

(a) Views of boundary-layer trips and heads of leading-edge attaching screws near upper tip of sharp leading edge.

Figure 3. Photographs showing portions of the sharp-leading-edge upper vertical fin.

Figure 3(b) shows the expansion-joint shields which covered the gaps between the leading-edge segments. The shields were constructed of 0.2-millimeter-(0.008-inch-) thick Inconel-X and were installed by wrapping them around the leading edge, to cover the gap, and spot welding them to one of the leading-edge segments. The combination

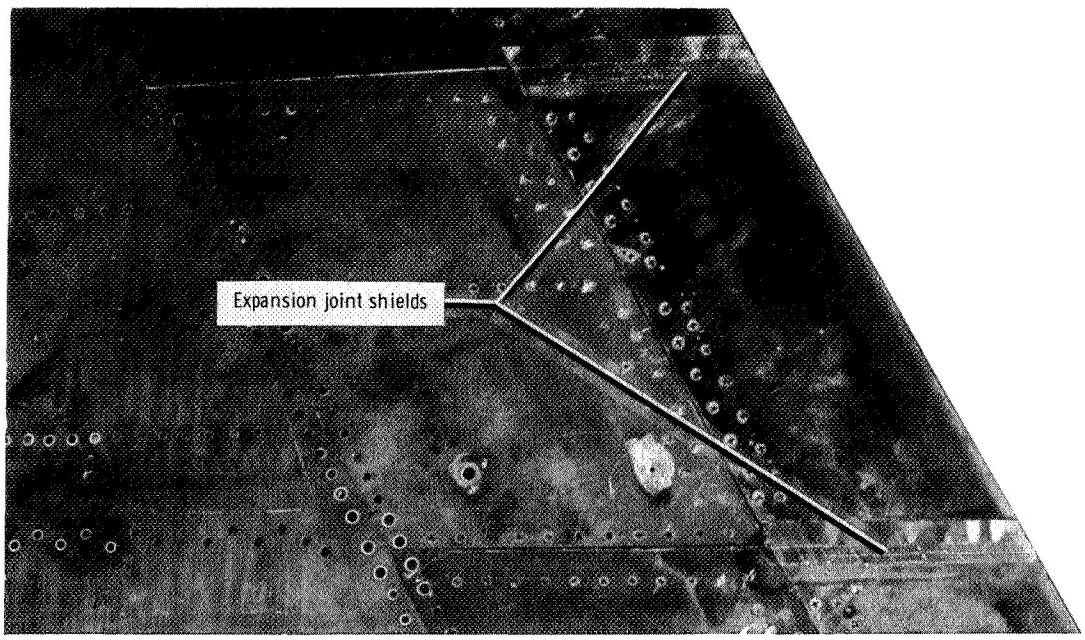

(b) Side view showing expansion joint shields.

Figure 3. Concluded.

of high flight temperatures and the attachment method caused permanent wavy protrusions in the shields. The amplitude of these protrusions in flight could not be determined, but it is thought that they were the largest protuberances on the surface.

Sensors

Pressure measurements were made on a small removable panel positioned aft of and slightly above the lower expansion joint on the vertical-tail surface (fig. 2). Figure 4 is a closeup view of the microphone, static-pressure orifice, and total-pressure probe installed on the panel. The total-pressure probe and static-pressure orifice were connected by flexible tubing to pressure transducers mounted on fin structural members behind the panel. Condenser microphones with diaphragm diameters of 0.483 centimeter (0.19 inch) and 0.31 centimeter (0.12 inch) were used in these tests (Photocon models No. 614 and No. 714). The microphone was flush mounted in the center of a 3.2-centimeter-(1.25-inch-) diameter block which was also flush mounted with the surface of the panel. The darker object on the block to the left of the microphone in figure 4 is a reference thermocouple, which was used to calibrate the microphone for transient heating.

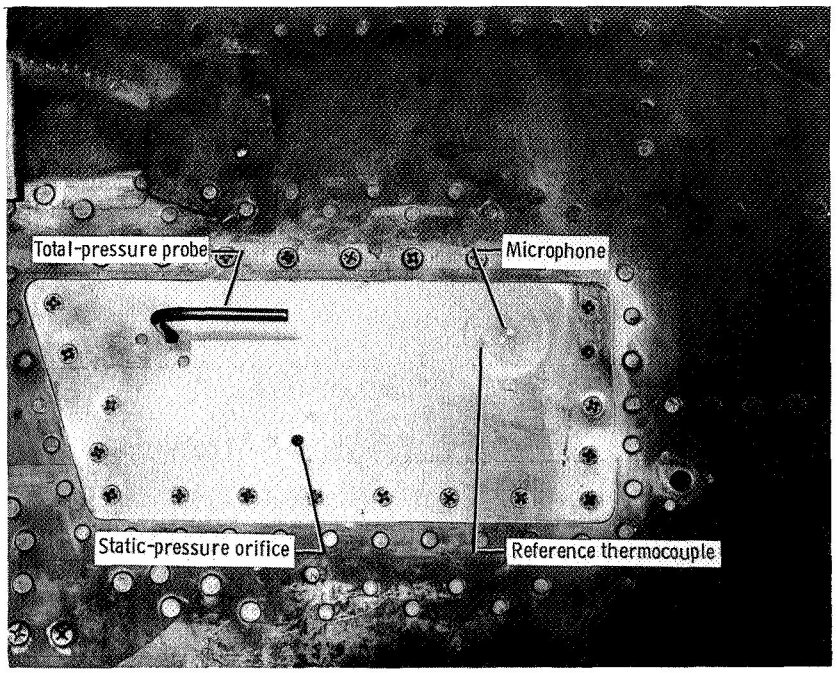

Figure 4. Closeup photograph of microphone and pressure sensor installation on the vertical fin.

Data System and Accuracy

The microphone and pressure transducer outputs were recorded on an airborne tape recorder. Subsequently, power-spectral-density estimates and overall sound pressure levels were obtained by an analog analysis using a Bruel & Kjaer octave band analyzer. A 1-second averaging time was used for the lowest octave band. The averaging times for the higher octaves were reduced, keeping the product of the averaging time and the filter bandwidth constant. This procedure resulted in power-spectral-density estimates with statistically equivalent accuracy.

The microphones used were calibrated for linearity and frequency response and for the effects of altitude, vibration, and steady-state and transient temperatures. These calibrations resulted in an estimated accuracy of ±3 decibels over a frequency range from 50 hertz to 10,000 hertz for all flight conditions. Details of the calibration procedures are presented in the appendix of reference 7, which describes the calibration of a 1.27-centimeter-(0.5-inch-) diameter microphone of the type used in these tests.

The total-pressure- and static-pressure-measuring transducers had ranges of 0 to 1030 hN/m^2 absolute (0 to 15 psia) and 0 to 345 hN/m^2 absolute (0 to 5 psia), respectively. Because of the high altitudes associated with these flight tests, pressure levels approached the lower limits of the transducer ranges for some of the flight test conditions and caused excessive errors in these measurements. The measured pressures were used only when the estimated error in the local dynamic pressure was less than ±3 percent. The corresponding errors in local Mach number and local unit Reynolds number were estimated to be ±6 percent and ±8 percent, respectively. When these estimated errors were exceeded, the local pressures and flow conditions were calculated by using the results of previous measurements on the fin (ref. 8), and the free-stream conditions. The free-stream conditions were determined from radar

speed and altitude measurements and from balloon and rocket soundings of the atmospheric conditions.

FLIGHT TEST CONDITIONS

The X-15 airplane was launched from a B-52 carrier aircraft at an altitude of about 13,700 meters (45,000 feet). For flights to high altitudes, an angle-of-attack-modulated climb was performed to establish the trajectory that would result in the desired speed and altitude conditions at engine burnout. A typical altitude flight time history is shown in figure 5. (Microphone data for this flight are presented later.) The times of interest

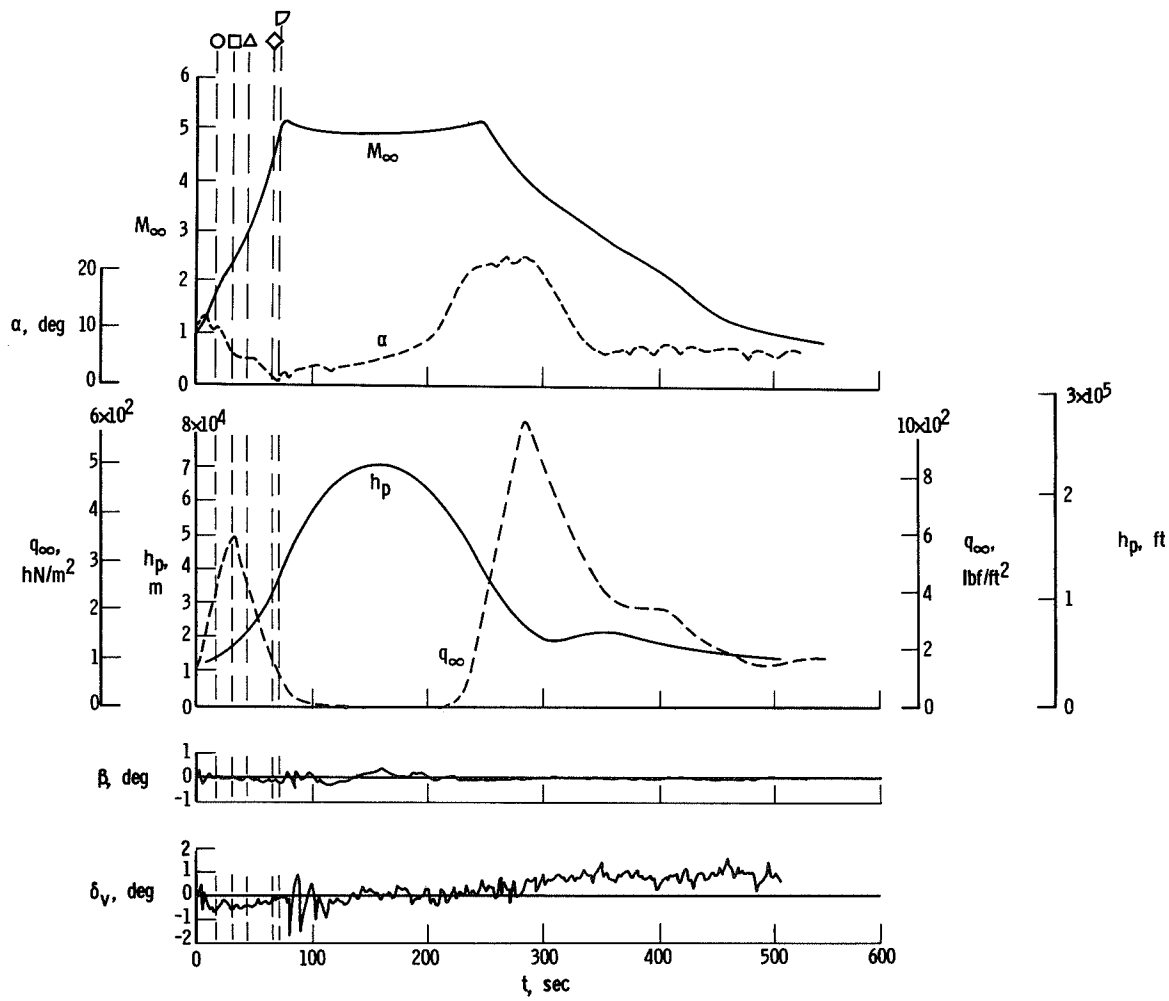

Figure 5. Time history of an X-15 high-altitude flight during which transition was detected on the vertical fin. Vertical dashed lines indicate times at which microphone data are correlated. Symbols identified in table 1.

in this report are identified by vertical dashed lines and symbols. Only data taken during the ascent portion of this and two other similar flights were correlated because the descending portion of the flights was characterized by high angles of attack, for which calculations of the vertical fin local-flow parameters would have been uncertain. The ascent produced relatively little heating, with the fin reaching temperatures typically near 373° K (672° R).

RESULTS AND DISCUSSION

Figure 6 presents time histories of the overall sound pressure level and the power-spectral-density estimates at the octave band center frequencies shown, which were measured on the vertical fin during the flight of figure 5. As explained in reference 9,

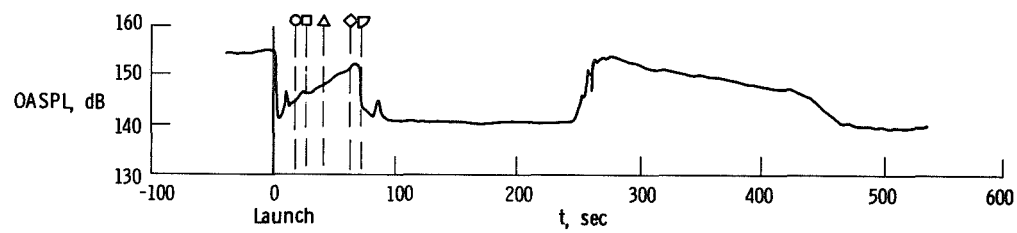

(a) Overall sound pressure level.

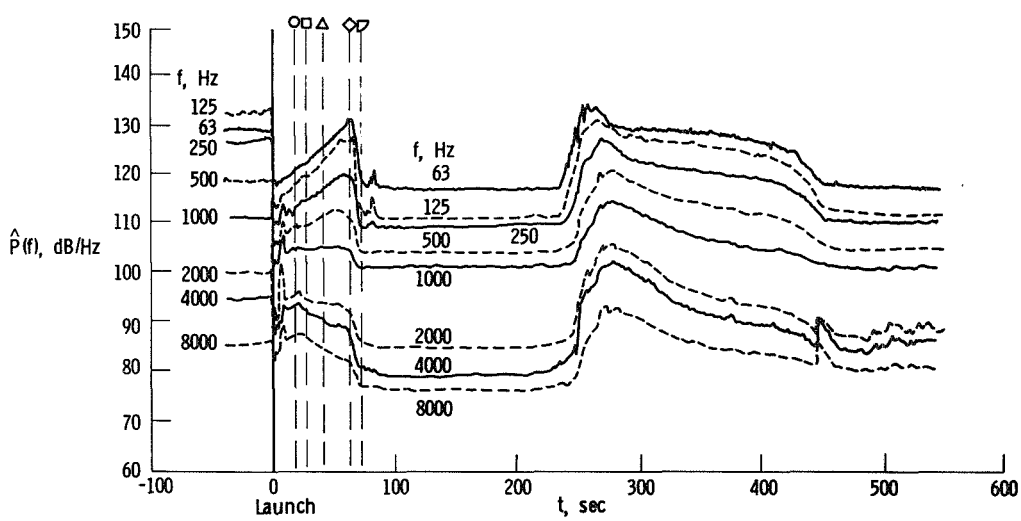

(b) Estimated power spectral density.

Figure 6. Time histories of the overall sound pressure level and the estimated power spectral density of the fluctuating surface pressure measured on the X-15 vertical fin during the high-altitude flight shown in figure 5. Vertical dashed lines indicate times at which the data are correlated. Symbols identified in table 1.

the overall sound pressure level was very high prior to launch because of aerodynamic interference with the B-52 carrier aircraft. At launch the level dropped to near the system noise levels (electrical background noise of the data system). As speed and altitude increased, the overall sound pressure level increased until a maximum was reached at $t = 75$ seconds; maximum free-stream Mach number was attained at $t = 78$ seconds. Thereafter, it dropped rapidly to the system noise level. For this particular flight, the sharp transient which occurred after the time indicated by the last vertical line is believed to have been caused by a rapid vertical fin deflection. Subsequently, there were other large deflections in the vertical fin, but because of the rapidly decreasing dynamic pressure, these deflections apparently were not sufficient to produce levels higher than system noise. The overall sound pressure level increased to a maximum again during the reentry phase of the flight (approximately $t = 280$ sec) and then gradually decreased during the decelerating glide to landing. These trends were typical of all high-altitude flights.

During ascent the lower frequency power-spectral-density estimates shown in figure 6 followed a trend similar to the overall sound pressure level; however, at the higher frequencies the trends in the power-spectral-density estimates were different. During the descent, the trends were similar in all frequencies. The spikes in the power-spectral-density estimates at higher frequencies just after launch and near the end of the flight were caused by the shock wave passing over the microphone as the aircraft passed through the sonic speed.

Pressure-Fluctuation Coefficients

At the times indicated by the vertical dashed lines and symbols, root-mean-square pressure-fluctuation coefficients, $\frac{\sqrt{\overline{p^2}}}{q_l}$, were formed by using the local dynamic pressure. These values are plotted against the local Reynolds number of the flow on the fin surface ($x = 85.4$ cm (33.7 in.)) in figure 7. Similar data from two additional flights are also shown. All fin data points are identified by the symbols in table 1.

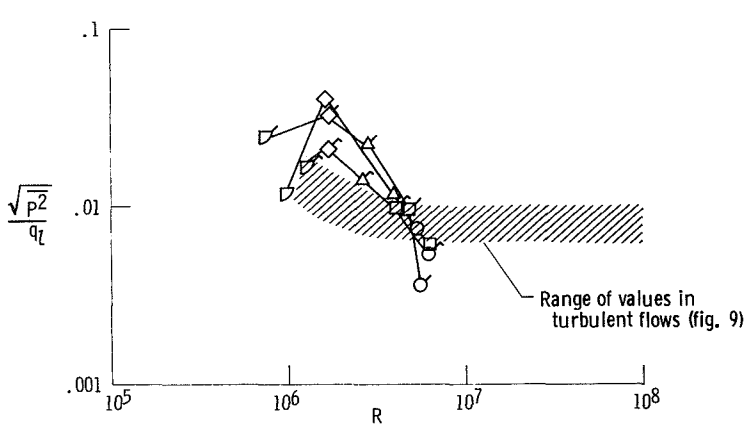

Figure 7. Root-mean-square pressure-fluctuation coefficients measured on the X-15 vertical fin during boundary-layer transition plotted against Reynolds number. Symbols identified in table 1.

TABLE 1.–ROOT-MEAN-SQUARE PRESSURE FLUCTUATIONS AND LOCAL FLOW PARAMETERS

Flight (a)	Symbol	$\sqrt{\overline{p^2}}$		q_l		M	$\frac{R}{x}$	
		hN/m^2	lbf/ft^2	hN/m^2	lbf/ft^2		m^{-1}	ft^{-1}
[b]3-51 (Photocon microphone No. 614)	○	1.44	2.99	190	396	1.4	[c]6.2×10^6	1.9×10^6
	□	1.82	3.82	287	600	1.8	[c]7.4	2.3
	△	2.97	6.21	252	525	2.7	4.4	1.4
	◇	4.64	9.74	112	233	3.7	1.9	.58
	▱	1.05	2.16	84	175	4.0	1.1	.34
3-53 (Photocon microphone No. 714)	○	1.10	2.29	306	640	1.5	[c]6.4×10^6	2.0×10^6
	□	3.45	7.18	354	740	2.7	[c]5.5	1.7
	△	9.82	20.5	431	910	4.7	[c]3.2	.97
	◇	8.28	17.3	250	522	4.6	1.9	.58
	▱	2.68	5.62	105	219	4.3	.84	.26
3-54 (Photocon microphone No. 714)	○	2.01	4.24	367	766	2.3	[c]6.9×10^6	2.1×10^6
	□	3.16	6.60	319	666	3.0	4.5	1.4
	△	3.93	8.15	268	559	3.5	3.0	.92
	◇	4.50	9.42	217	453	4.1	1.9	.58
	▱	3.11	6.48	179	374	4.6	1.5	.45

[a]In the flight designation system used for the X-15 airplanes, the first digit identifies the airplane and the following digits indicate the free-flight number.

[b]Typical flight shown in figure 5.

[c]Flow parameters derived from measured pressures.

As the Reynolds number decreased on the fin, the pressure-fluctuation coefficients increased to maximum values and then decreased. Maximum surface-pressure-fluctuation coefficients in the transition region are about an order of magnitude greater than those for fully developed turbulent flow. This trend is believed to be associated with the transition of the boundary layer from turbulent flow to laminar flow (sketch, fig. 8). Similar trends have been seen in surface-pressure-fluctuation data taken on a smooth cone in the transition region (ref. 10). These trends in the pressure fluctuations are also similar to those observed in surface shear, heat transfer rate, and equilibrium wall temperature in the transition region (refs. 11 to 15).

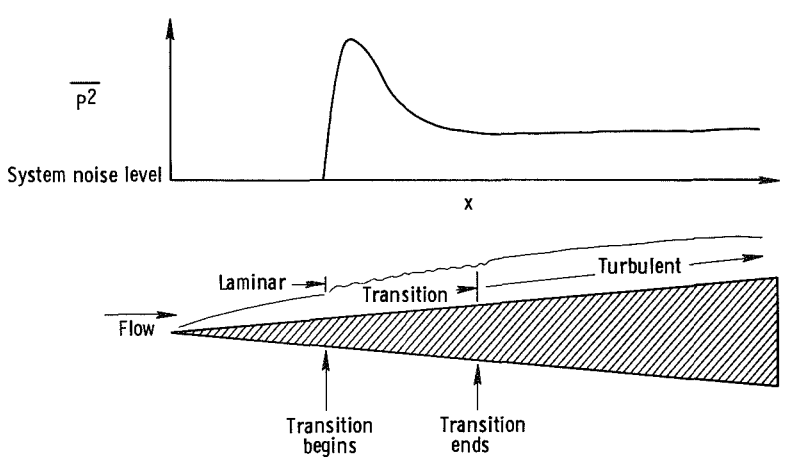

Figure 8. Sketch showing the implied mean square pressure variation in the boundary layer.

The Reynolds number at which the boundary layer on the fin changes from fully developed turbulent flow to transitional flow (i. e., the Reynolds number for the end of transition) was determined by comparing the fin data with pressure-fluctuation-coefficient data taken in either known or supposed turbulent flows. These data are shown in figure 9. The data were previously obtained on the X-15 fuselage (ref. 7) and on the XB-70 airplane. Also shown is the approximate range of surface-pressure-fluctuation coefficients found in incompressible turbulent flow on smooth plates in wind-tunnel tests. Except for some of the X-15 fuselage data at the lower Reynolds numbers, the turbulent-pressure-fluctuation coefficients, $\frac{\sqrt{\overline{p^2}}}{q_l}$, do not exceed a value of approximately 0.01. This level was taken as the upper limit for turbulent-pressure-fluctuation coefficients on the fin, and the Reynolds number for the end of transition on the fin was taken at the time this level was reached. Where the turbulent-pressure-fluctuation coefficients for the X-15 fuselage exceeded the 0.01 level at the lower Reynolds numbers, it is thought that the flow on the fuselage at that location was tending toward transition.

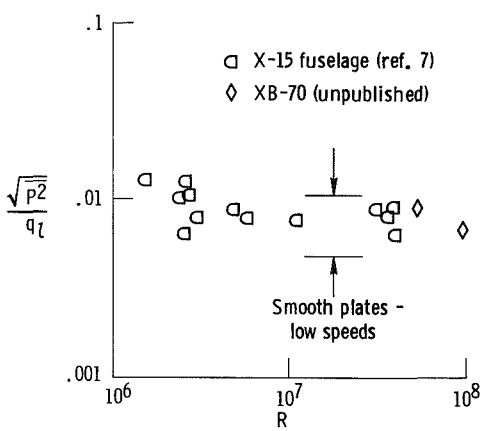

Figure 9. Root-mean-square pressure-fluctuation coefficients in turbulent flows plotted against Reynolds number.

As shown in figure 7, there was considerable scatter in the fin pressure-fluctuation coefficients at the lowest Reynolds numbers. This was probably due to errors associated with very low values of the local dynamic pressures combined with surface-pressure-fluctuation levels which were not much greater than the system noise level. This, unfortunately, precluded any attempt to establish the Reynolds numbers for the "beginning" of transition from these microphone data. The pressure-fluctuation coefficients for the "beginning" of transition are estimated, however, to be less than the lowest values given.

Transition Reynolds Numbers

The Reynolds numbers for the end of transition on the fin, determined as described previously, are compared with other data in figure 10. Shown for comparison are values obtained on flat plates in wind-tunnel tests using shadowgraph techniques (ref. 13), axial surface pitot pressure surveys (ref. 15), and surface heating rate analysis (ref. 12). Also shown is the Reynolds number for the end of transition on the X-15 vertical fin as determined from skin heating rates (ref. 16). The differences shown are not uncommon in experiments in which various detection techniques have been used (ref. 12). Also, a technique such as that used in this study can lead to considerable scatter in the data because all factors which could influence transition have not been accounted for (e. g., wall temperature, unit Reynolds number, stream turbulence, acoustic environment). For the purposes of this report, it is adequate to show that the Reynolds numbers for the end of transition on the vertical fin determined from surface-pressure-fluctuation measurements agree reasonably well with those determined in other experiments.

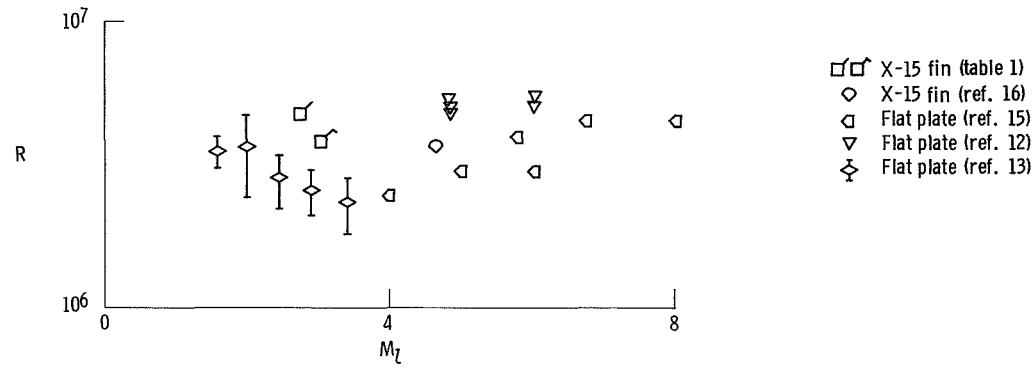

Figure 10. Reynolds numbers for the end of transition.

The peak values of the pressure-fluctuation coefficient on a smooth 10° cone with transition characteristics as described in reference 10 were found to be 0.02 and 0.1. The maximum values for the X-15 fin were within that range. However, the flow length Reynolds numbers for the maximum pressure-fluctuation coefficients on the smooth cone of reference 10 were greater than those on the vertical fin. In order to compare these values with other transition Reynolds numbers, the Reynolds numbers for the maximum values of the surface-pressure-fluctuation coefficients on the fin and cone are plotted in figure 11. Also shown are the Reynolds numbers for maximum surface shear on a flat plate (ref. 11) and the maximum Reynolds numbers for the beginning of transition on cones (ref. 14). Reynolds numbers equal to one-third the values for the beginning of transition found on cones are shown by the dashed line; these would be the values expected for the beginning of transition on flat plates if laminar stability theory were applicable.

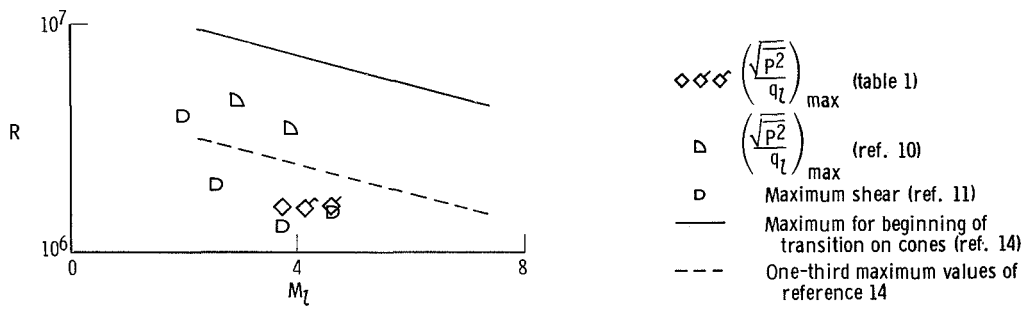

Figure 11. Other transition Reynolds numbers.

(The stability of the laminar flow depends upon the boundary-layer-thickness Reynolds number. For equal boundary-layer thickness, the length Reynolds number for stable laminar flow on cones would be three times greater than on flat plates.) If the Reynolds number for maximum surface-pressure-fluctuation coefficients is simply related to the Reynolds number for stable laminar flow, there is reason for the factor of three difference between the cone data of reference 10 and the vertical fin data of the present test. However, the Reynolds numbers for maximum surface-pressure fluctuations on the cone of reference 10 are less than the Reynolds numbers for the beginning of transition on cones from reference 14. Also, even though the vertical fin data compare favorably with the condition of maximum surface shear in reference 11, they are less than one-third the Reynolds numbers for the beginning of transition on the cones reported in reference 14. The reasons for these discrepancies are not known, but the differences may be due to factors not accounted for. Surface roughness placed on the fin was discounted as a possible factor as a result of a calculation made by using the

method of reference 17. The calculation gave the roughness height required to move transition forward of its natural position as being on the order of the boundary-layer thickness, which is a height greater than the measured roughness heights. However, the in-flight height of the leading-edge expansion joint shields could not be determined. It is possible, then, that the shields may have caused premature transition on the fin.

Estimated Power Spectral Density

The estimated power spectral density of the fin surface-pressure fluctuation is presented in figure 12 at the conditions given in table 1 for X-15 flight 3-51. These data were corrected for system noise. The system noise levels in each octave band are shown in figure 6(b) to be the approximately constant levels between 90 seconds and 220 seconds. The correction was made by subtracting the value of the mean square

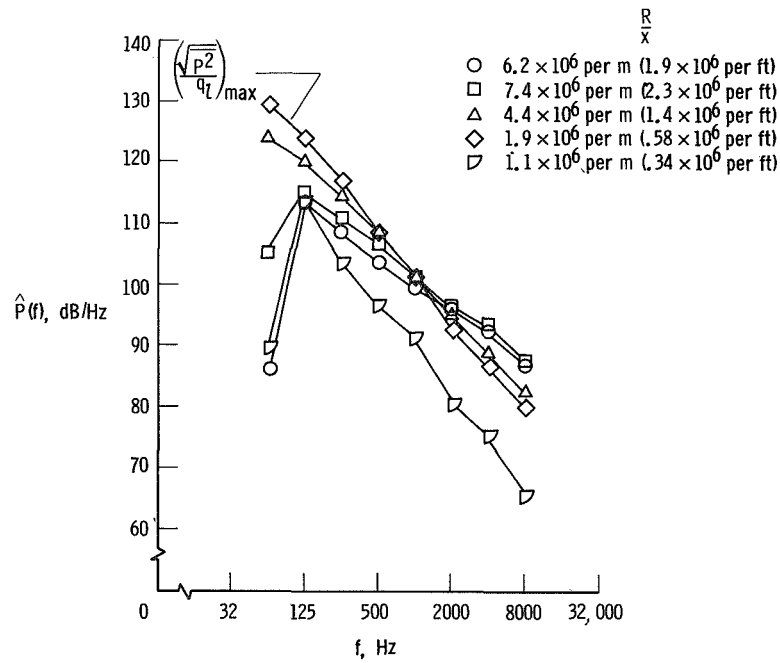

Figure 12. Estimated power spectral densities of the X-15 fin surface-pressure fluctuations evaluated at the times indicated in figure 6.

pressure during this time from the values at the times of interest, and then converting the difference to the decibel scale. As Reynolds number decreases in figure 12, the energy distribution of the surface-pressure fluctuation shifts from the higher frequencies to the lower frequencies. This shift continues up to the condition where the maximum root-mean-square pressure-fluctuation coefficient occurs, beyond which there is a major change in the level. At the last condition, which corresponds to the lowest Reynolds number, the power at all frequencies had diminished to about its lowest level. The largest change in the power-spectral-density estimates was about two orders of magnitude. The change occurred at 63 hertz at a time when it appeared that the boundary layer was changing from transitional to laminar flow (beginning of transition). A similar result was found from the measurements on the cone of reference 10.

CONCLUDING REMARKS

A microphone flush-mounted on the vertical fin of an X-15 airplane detected boundary-layer transition during flights in which a peak altitude of approximately 70,000 meters (230,000 feet) was reached. The results obtained provided a qualitative indication of the end of transition which agreed reasonably well with wind-tunnel data. The maximum surface-pressure-fluctuation coefficients in the transitional boundary layer on the X-15 fin were about an order of magnitude greater than in fully developed turbulent flow and were in general agreement with similar measurements from wind-tunnel tests on a cone. The frequency distribution of the surface-pressure fluctuations during transition was also similar, with a shift in the power from the high frequencies to the low frequencies as the boundary layer changed from turbulent to laminar flow. The greatest change in the power spectra occurred at the lowest frequencies and appeared to be the first indication of the beginning of transition on the fin.

Flight Research Center,
National Aeronautics and Space Administration,
Edwards, Calif., August 20, 1971.

REFERENCES

1. Banner, Richard D.; Kuhl, Albert E.; and Quinn, Robert D.: Preliminary Results of Aerodynamic Heating Studies on the X-15 Airplane. NASA TM X-638, 1962.

2. Braslow, Albert L.: Analysis of Boundary-Layer Transition on X-15-2 Research Airplane. NASA TN D-3487, 1966.

3. Mechtly, E. A.: The International System of Units - Physical Constants and Conversion Factors. NASA SP-7012, 1969.

4. Finch, Thomas W.; and Matranga, Gene J.: Launch, Low-Speed, and Landing Characteristics Determined From the First Flight of the North American X-15 Research Airplane. NASA TM X-195, 1959.

5. Banas, Ronald P.: Comparison of Measured and Calculated Turbulent Heat Transfer in a Uniform and Nonuniform Flow Field on the X-15 Upper Vertical Fin at Mach Numbers of 4.2 and 5.3. NASA TM X-1136, 1965.

6. Garringer, Darwin J.; and Saltzman, Edwin J.: Flight Demonstration of a Skin-Friction Gage to a Local Mach Number of 4.9. NASA TN D-3830, 1967.

7. Lewis, Thomas L.; and McLeod, Norman J.: Flight Measurements of Boundary-Layer Noise on the X-15. NASA TN D-3364, 1966.

8. McLain, L. J.; and Palitz, Murray: Flow-Field Investigations on the X-15 Airplane and Model Up to Hypersonic Speeds. NASA TN D-4813, 1968.

9. Jordan, Gareth H.; McLeod, Norman J.; and Guy, Lawrence D.: Structural Dynamic Experiences of the X-15 Airplane. NASA TN D-1158, 1962.

10. Pate, S. R.; and Brown, M. D.: Acoustic Measurements in Supersonic Transitional Boundary Layers. AEDC-TR-69-182, Arnold Eng. Dev. Center, Oct. 1969. (Available from DDC as AD694071.)

11. Coles, Donald: Measurements in the Boundary Layer on a Smooth Flat Plate in Supersonic Flow - III. Measurements in a Flat-Plate Boundary Layer at the Jet Propulsion Laboratory. Rep. No. 20-71, Jet Prop. Lab., Calif. Inst. Tech., June 1, 1953.

12. Holloway, Paul F.; and Sterrett, James R.: Effect of Controlled Surface Roughness on Boundary-Layer Transition and Heat Transfer at Mach Numbers of 4.8 and 6.0. NASA TN D-2054, 1964.

13. Chapman, Dean R.; Kuehn, Donald M.; and Larson, Howard K.: Investigation of Separated Flows in Supersonic and Subsonic Streams With Emphasis on the Effect of Transition. NACA Rep. 1356, 1958. (Supersedes NACA TN 3869.)

14. Mateer, George G.; and Larson, Howard K.: Unusual Boundary-Layer Transition Results on Cones in Hypersonic Flow. AIAA Paper No. 68-40, 1968.

15. Nagel, A. L.; Savage, R. T.; and Wanner, R. (With appendix by R. W. Blank): Investigation of Boundary Layer Transition in Hypersonic Flow at Angle of Attack. Tech. Rep. AFFDL-TR-66-122, Air Force Flight Dynamics Lab., Wright-Patterson Air Force Base, Aug. 1966.

16. Quinn, Robert D.; and Olinger, Frank V.: Flight-Measured Heat Transfer and Skin Friction at a Mach Number of 5.25 and at Low Wall Temperatures. NASA TM X-1921, 1969.

17. Braslow, Albert L.; Hicks, Raymond M.; and Harris, Roy V., Jr.: Use of Grit-Type Boundary-Layer-Transition Trips on Wind-Tunnel Models. NASA TN D-3579, 1966.

NASA-Langley, 1971 — 2 H-660

NATIONAL AERONAUTICS AND SPACE ADMISTRATION
WASHINGTON, D.C. 20546

OFFICIAL BUSINESS
PENALTY FOR PRIVATE USE $300

FIRST CLASS MAIL

POSTAGE AND FEES PAID
NATIONAL AERONAUTICS AND
SPACE ADMINISTRATION

U.S.MAIL

POSTMASTER: If Undeliverable (Section 158 Postal Manual) Do Not Return

"The aeronautical and space activities of the United States shall be conducted so as to contribute . . . to the expansion of human knowledge of phenomena in the atmosphere and space. The Administration shall provide for the widest practicable and appropriate dissemination of information concerning its activities and the results thereof."

— NATIONAL AERONAUTICS AND SPACE ACT OF 1958

NASA SCIENTIFIC AND TECHNICAL PUBLICATIONS

TECHNICAL REPORTS: Scientific and technical information considered important, complete, and a lasting contribution to existing knowledge.

TECHNICAL NOTES: Information less broad in scope but nevertheless of importance as a contribution to existing knowledge.

TECHNICAL MEMORANDUMS: Information receiving limited distribution because of preliminary data, security classification, or other reasons.

CONTRACTOR REPORTS: Scientific and technical information generated under a NASA contract or grant and considered an important contribution to existing knowledge.

TECHNICAL TRANSLATIONS: Information published in a foreign language considered to merit NASA distribution in English.

SPECIAL PUBLICATIONS: Information derived from or of value to NASA activities. Publications include conference proceedings, monographs, data compilations, handbooks, sourcebooks, and special bibliographies.

TECHNOLOGY UTILIZATION PUBLICATIONS: Information on technology used by NASA that may be of particular interest in commercial and other non-aerospace applications. Publications include Tech Briefs, Technology Utilization Reports and Technology Surveys.

Details on the availability of these publications may be obtained from:

SCIENTIFIC AND TECHNICAL INFORMATION OFFICE

NATIONAL AERONAUTICS AND SPACE ADMINISTRATION

Washington, D.C. 20546